Background removal in surface electron spectroscopy: Influence of surface excitations

Y. F. Chen
Precision Instrument Development Center, National Science Council, Hsinchu, Taiwan, Republic of China

Y. T. Chen
Department of Chemical Engineering, Wu Feng Institute of Technology & Commerce, Chiayi, Taiwan, Republic of China

(Received 20 April 1995; revised manuscript received 21 September 1995)

A deconvolution formula has been derived for the background subtraction of electron spectra by including the effect of surface excitations into the Landau formula. With this formula the primary x-ray photoelectron spectroscopy spectra of Cu, Ag, and Au are calculated from the experimental data. The primary excitation spectra are compared to the results derived by Tougaard's method in which surface effects were neglected. In all cases studied the present result is markedly different from Tougarrd's result which has a tail extending ~50 eV below the peak. It is found that the tail can be essentially removed when surface excitations are considered. In conclusion, the large tail which occurred in Tougaard's results is not part of the primary excitation spectrum but may be due to inelastically scattered electrons caused by surface excitations.

I. INTRODUCTION

X-ray photoelectron spectroscopy (XPS) and Auger electron spectroscopy (AES) are widely used to study the surface composition from the analysis of the emitted electron spectrum.[1,2] The surface sensitivity of these techniques comes from the very strong inelastic scattering of electrons in the 50–2000-eV range of primary importance. For this energy range, the electron inelastic mean free paths (IMFP's) typically range from a few to some tens of angstroms,[3–5] and unscattered electrons originate primarily from the outermost few atomic layers of the solid.

An important problem in quantitative analysis of the electron spectroscopy is the subtraction of the background intensity due to inelastically scattered electrons which accompanies each peak in the emitted electron spectrum.[6,7] In that way, the source energy distribution at the point of excitation in the solid may be determined, and compositional information may then be extracted. Several empirical methods have been proposed for subtraction of the background intensity.[8–11] Recently, many researchers[12–15] have used the transport equation to study this problem, and have derived a convenient deconvolution formula for the electron energy spectrum in the near-peak region. The general approach consists in employing Landau's formula[16] to describe the inelastic scattering process. In fact, Tougaard has applied this approach to derive the primary XPS spectra of Cu, Ag, and Au.[17,18] The resulting primary excitation spectra consist in all cases of a peak and a tail which extends ~50 eV below the peak energy. The tail was supposedly part of the primary excitation spectrum. However, Tougaard's method suffers a serious deficiency, i.e., the effect of surface excitations cannot be taken into account in the Landau formula. Recent studies on angle-resolved XPS and the reflection electron-energy-loss spectroscopy (REELS) (Refs. 19–21) have demonstrated that surface excitations are important for the electrons of energies ranging from a few to 2000 eV, and especially for electrons escaping at glancing angles. In addition, Hawn and DeKoven[22] have obtained a primary Au 4*f* XPS spectrum that has no large tail by the deconvolution procedure using experimental REELS spectra. It has, therefore, been open for discussion whether or not the true primary spectrum has a large tail.

In this work, we have included surface excitations into the Landau formula through Poisson statistics, and have derived a deconvolution formula in which the response function is in terms of the differential inverse mean free path (DIMFP) and the differential surface excitation parameter (DSEP). The DSEP for electrons passing obliquely through solid surfaces was derived including the recoil effect without the small-angle approximation. A model dielectric function[5] developed previously has been employed to calculate the DIMFP's and DSEP's. Applying the calculated cross sections into the modified Landau formula, we have calculated the primary XPS excitation spectra of Cu, Ag, and Au form the experimental data. The results revealed that the influence of surface excitations on the background removal of the spectra is considerably significant for the energy range ~50 eV below the peak energy. It was also found that the large tail which occurred in Tougaard's results can almost be removed when surface excitations are considered.

II. INELASTIC INTERACTIONS OF AN ELECTRON EMITTED FROM A SOLID SURFACE

Plasmon excitations, which are the most important inelastic interactions between emitted electrons and solid electrons in the medium, comprise mainly bulk and surface excitations. Electrons near a surface are primarily responsible for surface excitations, while those deep inside contribute mostly to bulk excitations. Both bulk and surface excitations can be described in terms of the dielectric function of the solid.

Although the specular-reflection model introduced by Ritchie and Marusak[23] is known to reproduce many properties of real surfaces very well, a knowledge of the electrodynamics of nonspecular surfaces is needed in the case of XPS. In this work, we shall study the inelastic interactions of an

electron emitted from a solid surface. The surface will be chosen at the plane $z=0$, with the z axis in the perpendicular direction from the solid $\varepsilon(\mathbf{q},\omega)$ to the vacuum. The notations $\nu=|\boldsymbol{\nu}|$, $\mathbf{q}=(\mathbf{Q},q_z)$, $\boldsymbol{\nu}=(\boldsymbol{\nu}_\parallel,\nu_z)$, and $\mathbf{r}=(\mathbf{R},z)$, where $\mathbf{Q}$, $\boldsymbol{\nu}_\parallel$, and $\mathbf{R}$ represent the corresponding components parallel with the surface, will be adopted hereafter. Note that atomic units are used through this work, unless otherwise specified.

For an electron with the velocity $\boldsymbol{\nu}$ crossing the surface at $t=0$ from the solid $\varepsilon(\mathbf{q},\omega)$ to the vacuum, the Fourier components of the scalar electric potential are given by

$$\phi^{(s)}(\mathbf{q},\omega)=\frac{-8\pi^2}{q^2\varepsilon(\mathbf{q},\omega)}[\,\delta(\omega-\mathbf{q}\cdot\boldsymbol{\nu})+\rho_s(\mathbf{Q},\omega)], \quad z<0, \tag{1}$$

$$\phi^{(\nu)}(\mathbf{q},\omega)=\frac{-8\pi^2}{q^2}[\,\delta(\omega-\mathbf{q}\cdot\boldsymbol{\nu})-\rho_s(\mathbf{Q},\omega)], \quad z>0. \tag{2}$$

The first terms in Eqs. (1) and (2) represent the charge density of the moving electron, and $\rho_s(\mathbf{Q},\omega)$ is the amplitude of the fictitious surface charge necessary to satisfy the requisite boundary conditions, respectively. The opposite sign of the second term between Eqs. (1) and (2) originates from the requirement of continuity of the electric displacement. The continuity of the potential at the surface yields $\rho_s(\mathbf{Q},\omega)$ as

$$\rho_s(\mathbf{Q},\omega)=\frac{Q}{\pi}\frac{|\nu_z}{\tilde{\omega}^2+(\nu_z Q)^2}\frac{\bar{\varepsilon}(\mathbf{Q},\omega)}{\varepsilon(\tilde{\mathbf{q}},\omega)}\frac{\varepsilon(\tilde{\mathbf{q}},\omega)-1}{\bar{\varepsilon}(\mathbf{Q},\omega)+1}, \tag{3}$$

where

$$\frac{1}{\bar{\varepsilon}(\mathbf{Q},\omega)}=\frac{Q}{\pi}\int_{-\infty}^{\infty}\frac{dq_z}{q^2\varepsilon(\mathbf{q},\omega)}, \tag{4}$$

$\tilde{\omega}=\omega-\boldsymbol{\nu}\cdot\mathbf{Q}$ and $\tilde{q}^2=Q^2+\tilde{\omega}^2/\nu_z^2$. From Eqs. (1) and (2), and in terms of $\rho_s(\mathbf{Q},\omega)$, the induced scalar potential can be expressed as

$$\phi_{\rm ind}(\mathbf{r},t)=\frac{-1}{2\pi^2}\int d\omega\int d^3\mathbf{q}\,\frac{e^{i(q\cdot r-\omega t)}}{q^2}\times\left\{\rho_s(\mathbf{Q},\omega)\left[\frac{\Theta(-z)}{\varepsilon(\mathbf{q},\omega)}-\Theta(z)\right]+\delta(\omega-\mathbf{q}\cdot\boldsymbol{\nu})\times\Theta(-z)\left[\frac{1}{\varepsilon(\mathbf{q},\omega)}-1\right]\right\}, \tag{5}$$

where $\Theta(z)$ is the Heaviside step function.

The retarding force, which can be interpreted as a space-dependent stopping power, is given by[24]

$$-\frac{dW}{ds}=\frac{1}{\nu}\left[\frac{\partial\phi_{\rm ind}(\mathbf{r},t)}{\partial t}\right]_{r=\nu t}, \tag{6}$$

where the derivative of $\phi_{\rm ind}$ is evaluated at the position of the electron, $\mathbf{r}=\nu t$. From Eqs. (5) and (6), after some algebra, we obtain the stopping power of the solid for the electron:

$$-\frac{dW}{dS}=\frac{i}{2\pi^2\nu}\int\omega\,d\omega\int d^2\mathbf{Q}\left\{\frac{\pi}{Q}\rho_s(\mathbf{Q},\omega)e^{-i\tilde{\omega}z/\nu_z}\left[\frac{\Theta(-z)}{\bar{\varepsilon}(\mathbf{Q},\omega,z)}-e^{-Q|z|}\Theta(z)\right]+\frac{|\nu_z|}{\tilde{\omega}^2+(\nu_z Q)^2}\Theta(-z)\left[\frac{1}{\varepsilon(\tilde{\mathbf{q}},\omega)}-1\right]\right\}, \tag{7}$$

where

$$\frac{1}{\bar{\varepsilon}(z,\mathbf{Q},\omega)}=\frac{Q}{\pi}\int_{-\infty}^{\infty}\frac{dq_z e^{iq_z z}}{q^2\epsilon(q,\omega)} \tag{8}$$

The first term inside the curly bracket of Eq. (7) represents the surface contribution, while the other term is the usual bulk contribution. The evaluation of the first term in Eq. (7) depends on sign z, as this determines whether the ω integration must be performed by closing through the upper (U) or lower (L) half-plane (HP). For $z<0$, i.e, the electron inside the solid $\epsilon(\mathbf{q},\omega)$ and approaching the surface, we must close the integration contour through the UHP. On the other hand, for $z>0$, i.e., the electron inside the vacuum and moving away from the surface, the integration contour must be closed through the LHP. This integration contour involves the poles of $\rho_s(\mathbf{Q},\omega)$ and $1/\bar{\varepsilon}(\mathbf{Q},\omega,z)$ which approach the real axis from below and give the surface and bulk excitation modes of the solid, respectively. For simplicity it is convenient to use the identity[25]

$$e^{-i\tilde{\omega}z/\nu_z}=2\cos(\tilde{\omega}z/\nu_z)-e^{i\tilde{\omega}z/\nu_z}. \tag{9}$$

The integration containing the complex exponential on the right-hand side of Eq. (9) can then be performed again through the UHP. Therefore Eq. (7) can be written as

$$-\frac{dW}{ds}=\frac{1}{\pi^2\nu}\int_0^\infty d\omega\int d^2\mathbf{Q}\,\frac{\omega|\nu_z|}{\tilde{\omega}^2+(\nu_z Q)^2}\times\mathrm{Im}\left[\Pi(\boldsymbol{\nu},z,\mathbf{Q},\omega)-\frac{\Theta(-z)}{\varepsilon(\tilde{\mathbf{q}},\omega)}\right], \tag{10}$$

where

$$\Pi(\nu,z,\mathbf{Q},\omega)=e^{-Q|z|}\left[\frac{\Theta(-z)}{\bar{\epsilon}(z,\mathbf{Q},\omega)}-[2\cos(\tilde{\omega}z/\nu_z)-e^{-Q|z|}]\Theta(z)\right]\left[-\frac{\bar{\varepsilon}(\mathbf{Q},\omega)}{\varepsilon(\tilde{\mathbf{q}},\omega)}\frac{\varepsilon(\tilde{\mathbf{q}},\omega)-1}{\bar{\varepsilon}(\mathbf{Q},\omega)+1}\right] \tag{11}$$

corresponds to the spatially varying surface energy-loss function. In this derivation we have used the property $\varepsilon(-\mathbf{q},-\omega)=\varepsilon^*(\mathbf{q},\omega)$.

For an electron of energy $E=\nu^2/2$ to loss energy ω, the spatially varying differential inverse mean free path (DIMFP), $\mu(E\rightarrow E-\omega,\alpha,z)$, can be related to stopping power as follows:

$$-\frac{dW}{ds}=\int_0^\infty \omega\mu(E\rightarrow E-\omega,\alpha,z)d\omega, \tag{12}$$

where α is the electron emission angle with respect to the surface normal. The definition of α will be used hereafter. From Eqs. (10)–(12), the DIMFP for electrons emitted from the surface can be split up into a bulk and a surface term,

$$\mu(E\rightarrow E-\omega,\alpha,z)=\mu_B(E\rightarrow E-\omega)+\mu_s(E-dE-\omega,\alpha,z), \tag{13}$$

where

$$\mu_B(E\rightarrow E-\omega)=\frac{1}{\pi^2\nu}\int d^2\mathbf{Q}\,\frac{|\nu_z|}{\tilde{\omega}^2+(\nu_z Q)^2}\,\mathrm{Im}\left[-\frac{\Theta(-z)}{\varepsilon(\tilde{\mathbf{q}},\omega)}\right] \tag{14}$$

and

$$\mu_s(E\rightarrow E-\omega,\alpha,z)=\frac{1}{\pi^2\nu}\int d^2\mathbf{Q}\,\frac{|\nu_z|}{\tilde{\omega}^2+(\nu_z Q)^2}\,\mathrm{Im}[\Pi(\boldsymbol{\nu},z,\mathbf{Q},\omega)]. \tag{15}$$

The bulk term, which is independent of the position and emission angle, gives rise to the well-known expression of the DIMFP of electrons moving in an infinite medium.[26] On the other hand, the surface term is z and α dependent. Since there is the $e^{-Q|z|}$ term in $\Pi(\boldsymbol{\nu},\mathbf{z},\mathbf{Q},\omega)$, the surface quasimode has a rather limited extent about the surface. The effective region extends into the solid to a depth about ν/ω_p, where ω_p is the plasmon energy.[27] The depth is roughly around 3–6 Å for a 1-keV electron from the fact that ω_p lies in the interval 20–35 eV. Accordingly, in XPS, where the concentration of excited electrons is likely homogeneous, we may expect that most emitted electrons penetrate the effective region of surface excitations. Thus surface effects can be approximately characterized by the differential surface excitation parameter (DSEP) (Ref. 27) which can be calculated via integration of Eq. (15), i.e.,

$$P_s(E\rightarrow E-\omega,\alpha)=\int_{-\infty}^{\infty}\frac{dz}{\cos\alpha}\,\mu_s(E\rightarrow E-\omega,\alpha,z). \tag{16}$$

The surface excitation parameter (SEP) for an electron crossing a vacuum-solid surface is then given by[27]

$$P_s(E,\alpha)=\int_0^E P_s(E\rightarrow E-\omega,\alpha)d\omega. \tag{17}$$

Neglecting the effect of spatial dispersion of the medium, a local dielectric function $\epsilon(\omega)$ could be used to describe the response of the medium. From Eqs. (4) and (8) we easily obtain

$$\bar{\varepsilon}(\mathbf{Q},\omega)=\varepsilon(\tilde{q},\omega)=\varepsilon(\omega) \tag{18}$$

and

$$\bar{\varepsilon}(z,\mathbf{Q},\omega)=\varepsilon(\omega)e^{Q|z|} \tag{19}$$

Carrying out the integration over $\mathbf{Q}$ and z in Eq. (17), we obtain

$$P_s(E,\alpha)=\frac{1}{2\nu(\cos\alpha)}\int_0^E\frac{d\omega}{\omega}\,\mathrm{Im}\left[\frac{(1-\varepsilon)^2}{\varepsilon(1+\varepsilon)}\right]. \tag{20}$$

Substituting the free-electron-gas dielectric function

$$\varepsilon(\omega)=1-\frac{\omega_P^2}{\omega(\omega+i\gamma)},\quad \gamma\rightarrow 0^+ \tag{21}$$

into Eq. (18), we obtain

$$P_s(E,\alpha)=\frac{\pi}{4\nu}\frac{1}{\cos\alpha}. \tag{22}$$

This shows that the surface excitation probability is proportional to $(\cos\alpha)^{-1}$. This angular dependence has been verified experimentally for a large-α value. Taking $\alpha=0°$ in Eq. (22), we obtain the results of Ritchie[26] for normal incident electrons.

So far, the recoil effect is neglected in the derivation. Based on the conservation of energy and momentum, this effect can be included by limiting the range of integration over $\mathbf{Q}$ as follows:

$$q_-^2\leqslant\left(\frac{\tilde{\omega}}{\nu_z}\right)^2+Q^2\leqslant q_+^2, \tag{23}$$

where $q_\pm=\sqrt{2E}\pm\sqrt{2(E-\omega)}$.

The model dielectric used in this work is identical to that used previously. Here we present a brief synopsis for the purpose of completeness. The real and imaginary parts of the dielectric function are given by[5,28–30]

$$\varepsilon_1(q,\omega)=\varepsilon_b-\sum_i\frac{A_i[\omega^2-(\omega_i+q^2/2)^2]}{[\omega^2-(\omega_i+q^2/2)^2]^2+(\omega\gamma_i)^2} \tag{24}$$

and

$$\varepsilon_2(q,\omega)=\sum_i\frac{A_i\gamma_i\omega}{[\omega^2-(\omega_i+q^2/2)^2]^2+(\omega\gamma_i)^2}, \tag{25}$$

where A_i, γ_i, and ω_i, respectively, are the oscillator strength, damping coefficient, and critical-point energy, all associated with the ith interband transition. Note that we include an ε_b term to account for the background dielectric constant due to the influence of polarizable atomic cores.[31] Since the exact dependence of the dielectric function on the momentum transfer is seldom known, an extrapolation from the optical limit to other momentum transfers must be made. The expression adopted in Eqs. (24) and (25) for the q dependence works correctly at the two ends of the momentum transfer, i.e., $q\rightarrow 0$ and $q\rightarrow\infty$, with an accuracy proportional to q^2.[30] The actual dispersion relation makes only a minor difference in the determination of the DIMFP and DSEP.[32,33]

The parameters in the model dielectric function were determined by a fit of Eq. (25), in the limit $q\rightarrow 0$, to the experimental optical data. To make sure that the fitted param-

eters are accurate, we require that the model dielectric function satisfies two sum rules, i.e.,

$$\int_0^{\hat{\omega}} \omega \varepsilon_2(0,\omega) d\omega = \frac{\pi}{2} \sum_i A_i = \frac{\pi}{2} \omega_p^2 \tag{26}$$

and

$$\int_0^{\hat{\omega}} \omega \ \mathrm{Im}\left[\frac{-1}{\varepsilon(0,\omega)}\right] d\omega = \frac{\pi \omega_p^2}{2\varepsilon_b^2}, \tag{27}$$

where ω_p is the bulk plasmon energy of valence electrons, and $\hat{\omega}$ is an energy cutoff, large compared to the valence-band excitations but well below the energy of the inner-shell transitions responsible for the dispersive dielectric background.

III. DECONVOLUTION FORMULA

In general, it is difficult to obtain an analytical solution because of the correlation between energy and angle scattering cross sections involved in the equation. However, it is reasonable to assume that only elastic interactions contribute to the angular deflection, and only inelastic interactions contribute to the energy loss. With this assumption, the flux of electrons $J(E,\vec{\Omega})dE\ d^2\Omega$ emitted from the solid surface with energy (E,dE) in solid angle $(\vec{\Omega},d^2\Omega)$ is given by[12,34]

$$J(E,\vec{\Omega}) = \int dE_0 F(E_0) \int dx' f(x') \int d^2\Omega_0 \int dR \times Q(E_0,\vec{\Omega}_0,x';R,\vec{\Omega}) G(E_0,R;E,\vec{\Omega}), \tag{28}$$

where $G(E_0,R;E,\vec{\Omega})$ is the energy distribution of an electron of initial energy E_0 after having traveled the path length R; $Q(E_0,\vec{\Omega},x';R,\vec{\Omega})$ is the angular and path length distribution of an electron, excited isotropically at depth x' to a kinetic energy E_0, passing the surface in a direction $(\vec{\Omega},d^2\Omega)$; and $F(E_0)$ is the source energy distribution of excited electrons, assumed to be uncorrelated with the depth distribution $f(x')$ of the excited electron.

In the case of a homogeneous concentration of excited electrons, which is likely in XPS and photonexcited AES where the source attenuation is negligible, the path length distribution may be expressed by a single exponential[13]

$$\int_0^{\infty} dx' Q(E_0,\vec{\Omega}_0,x';R,\vec{\Omega}) f(x') = I(\vec{\Omega}) e^{-R/L}. \tag{29}$$

Here L is the characteristic attenuation length, and $I(\vec{\Omega})$ is the angular distribution. Within the $P1$ approximation to the Boltzmann transport equation, $L \approx 5.6\lambda_t$, λ_t is the transport mean free path for elastic scattering. To obtain a more accurate characteristic attenuation length, the path-length distribution may be obtained by resorting to the Monte Carlo simulation on the basis of a quasielastic model. With this path-length distribution, the energy spectrum is then given by

$$J(E,\vec{\Omega}) = I(\vec{\Omega}) \int dE_0 F(E_0) \int e^{-R/L} G(E_0,R;E,\vec{\Omega}) dR. \tag{30}$$

For the energy spectrum near a peak, the range of the path length, R, is of the order of several times the value of the IMFP, λ. Since in general $\lambda \ll L$, the influence of angular electron deflection on the energy spectrum near-peak region can be ignored.[34] This conclusion indicates that a detailed description of inelastic scattering in the function $G(E_0,R;E,\vec{\Omega})$ is far more important for the determination of the energy spectrum of emitted electrons in the near-peak region compared to the effect of angular deflection on the function Q.

The energy-loss distribution is often given by Landau's formula[16]

$$G_L(E_0,R;E) = \frac{1}{2\pi} \int_{-\infty}^{\infty} ds\ \exp[is\omega - R\Sigma(E_0;s)], \tag{31}$$

with

$$\Sigma(E_0;s) = \int_0^{\infty} d\omega\ \mu_B(E_0 \to E_0-\omega)[1-\exp(-is\omega)] = \frac{1}{\lambda_B(E_0)} - \tilde{\mu}_B(E_0;s), \tag{32}$$

where $\omega = E_0 - E$, $\tilde{\mu}_B(E_0;s)$ is the Fourier transform of $\mu_B(E_0 \to dE_0-\omega)$ with respect to ω, and $\lambda_B(E_0)$, the IMFP of bulk excitations, is given by

$$\lambda_B^{-1}(E_0) = \int_0^{E_0} \mu_B(E_0 \to E_0-\omega) d\omega. \tag{33}$$

Note that the Landau formula is independent of the escape angle of electrons due to the isotropic property of the bulk excitations.

The energy-loss distribution contributed by surface excitations can be explained in terms of the DSEP. Note that the DSEP is the probability for a single loss event. For the total surface loss spectrum, we therefore have to sum over all multiple loss events using[35–38]

$$G_s(E_0,\alpha;E) = \int_0^{\infty} ds\ \exp[is\omega - \Xi(E_0,\alpha;s)] \tag{34}$$

and

$$\Xi(E_0,\alpha;s) = \int_0^{\infty} d\omega\ P_s(E_0 \to E_0-\omega,\alpha)[1-\exp(-is\omega)] = P_s(E_0,\alpha) - \tilde{P}_s(E_0,\alpha;s), \tag{35}$$

where $\tilde{P}_s(E_0,\alpha;s)$ is the Fourier transform of $P_s(E_0 \to E_0-\omega,\alpha)$ with respect to ω.

Expanding the exponential term $\exp[-\Xi(E_0,\alpha;s)]$, in Eq. (34), we obtain

$$\exp[-\Xi(E_0,\alpha;s)] = \exp[-P_s(E_0,\alpha)] \times \sum_{n=0}^{\infty} \frac{[\tilde{P}_s(E_0,\alpha;s)]^n}{n!}, \tag{36}$$

which is the result of the Poisson stochastic process for surface excitations.

Using the convolution method, we can incorporate the surface effect into the Landau formula and find the total energy-loss distribution

$$G(E_0,\alpha,R;E)=\int_0^{E_0} G_L(E_0,R;E')G_s(E',\alpha;E)dE'. \quad (37)$$

The product term on the right-hand side of Eq. (37) represents that an electron of initial energy E_0 loses energy E_0-E' due to bulk excitations, and loses energy $E'-E$ due to surface excitations. From the convolution theorem of the Fourier transform and Eqs. (31) and (34), $G(E_0,\alpha,R;E)$ can be written as

$$G(E_0,\alpha,R;E)=\frac{1}{2\pi}\int_{-\infty}^{\infty} ds\ \exp[is\omega-R\Sigma(E_0;s) -\Xi(E_0,\alpha;s)] \quad (38)$$

Using Eqs. (32) and (35) and expanding $G(E_0,\alpha,R;E)$ in Eq. (38), we can find

$$G(E_0,\alpha,R;E)=e^{-[R/\lambda_B(E_0)+P_s(E_0,\alpha)]}\Bigg[\delta(E_0-E)+R\mu_B(E_0\to E)+P_s(E_0\to E,\alpha)+\int R\mu_B(E_0\to\tilde{E})P_s(\tilde{E}\to E,\alpha)d\tilde{E} +\frac{1}{2!}R^2\int \mu_B(E_0\to E')\mu_B(E'\to E)dE'+\frac{1}{2!}\int P_s(E_0\to E',\alpha)P_s(E'\to E,\alpha)dE'+\cdots\Bigg], \quad (39)$$

where the first, second, third, etc. terms in the bracket represent, respectively, the energy-loss flux due to a zero plasmon, bulk plasmon, a surface plasmon, a bulk plasmon and surface plasmon, two bulk plasmons, etc. This expression indicates that $G(E_0,\alpha,R;E)$ in Eq. (38) includes all multiple-loss events contributed by bulk and surface excitations.

Substituting Eq. (38) into Eq. (30), and carrying out the integration over R, we obtain

$$J(E,\vec{\Omega})=\frac{L\lambda_B}{L+\lambda_B}I(\vec{\Omega})e^{-P_s(E_0,\alpha)}\Bigg[F(E)+\int_E^{\infty}F(E_0)\times A(E_0\to E,\alpha)dE_0\Bigg] \quad (40)$$

and

$$A(E_0\to E,\alpha)=\frac{1}{2\pi}\int_{-\infty}^{\infty} ds\ \exp[i(E_0-E)s]\times\left\{\frac{\exp[\tilde{P}_s(E_0,\alpha;s)]}{1-\frac{L\lambda_B}{L+\lambda_B}\tilde{\mu}_B(E_0;s)}-1\right\}. \quad (41)$$

Here $A(E_0\to E,\alpha)$, the response function, describes specimen interactions. With the obtained DIMFP and DSEP, the response function can be calculated rapidly using the fast Fourier transform (FFT) algorithm. Usually, only relative intensity measurements will be performed. Hence, introducing the relative electron flux density distribution

$$j(E,\alpha)=\left[\frac{L\lambda_B}{L+\lambda_B}I(\vec{\Omega})e^{-P_s(E_0,\alpha)}\right]^{-1}J(E,\vec{\Omega}), \quad (42)$$

we can write Eq. (40) in the general form

$$j(E,\alpha)=\left[F(E)+\int_E^{\infty}F(E_0)A(E_0\to E,\alpha)dE_0\right]. \quad (43)$$

It is noted that the response function is dependent on the emission angle due to inclusion of the surface excitations. Taking $P_s(E_0\to E_0-\omega,\alpha)=0$, i.e., neglecting the surface effects, we find that Eq. (41) reduces to the result of Tofterup.[13,15]

For a numerical treatment, a maximum kinetic energy $E_{\max}$ is chosen to lie a few eV on the high-energy side of the peak structure. Dividing the spectrum below $E_{\max}$ into channels $E_i=E_{\max}-i\Delta E$, we then find a recursion formula for the determination of $F(E)$,

$$F(E_i)=j(E_i,\alpha)-\sum_{m=1}^{i-1}F(E_m)A(E_m\to E_i,\alpha)\Delta E, \quad (44)$$

where $i=1,2,3\ldots$ is the space index, and ΔE is the mesh size. Hence once $j(E,\alpha)$ and $A(E_0\to E,\alpha)$ are given, and the source function $F(E)$ with background subtracted is then obtained by the recursion formula.

IV. RESULTS AND DISCUSSION

On the basis of the model dielectric function, we have calculated the DIMFP for bulk excitations and the DSEP for surface excitations. The parameters in the model dielectric function have been obtained in our previous works.[5,32,33] A plot of the energy-loss dependence of the calculated DIMFP's for electrons with various energies in Cu, Ag, and Au is shown in Fig. 1. As the energy is increased, the DIMFP's for bulk excitations in general decreases, as one would expect. However, the structures and peak positions of DIMFP's for different electron energies are similar.

Figure 2 shows a plot of the DSEP's for electrons of several energies that escape normally from Cu, Ag, and Au as a function of the energy loss. As for the DIMFP's, the DSEP's decrease with increasing electron energy, and the observed structure and peak positions of these curves are insensitive to the electron energy. It is seen that surface excitations contribute largely at small energy losses as compared to bulk excitations.

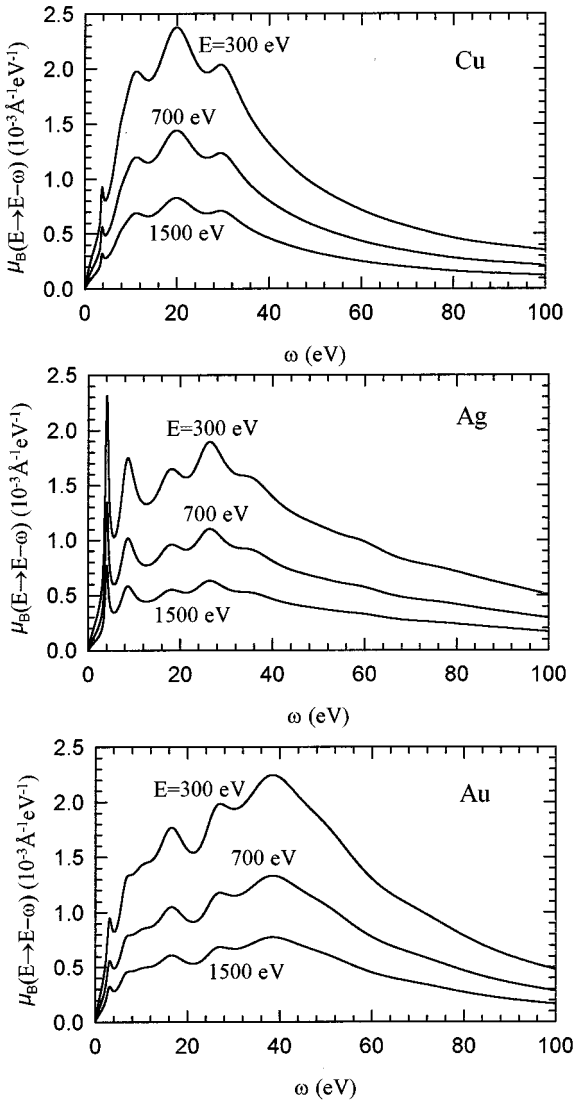

FIG. 1. A plot of the energy-loss dependence of the calculated DIMFPs for electrons with various energies in Cu, Ag, and Au.

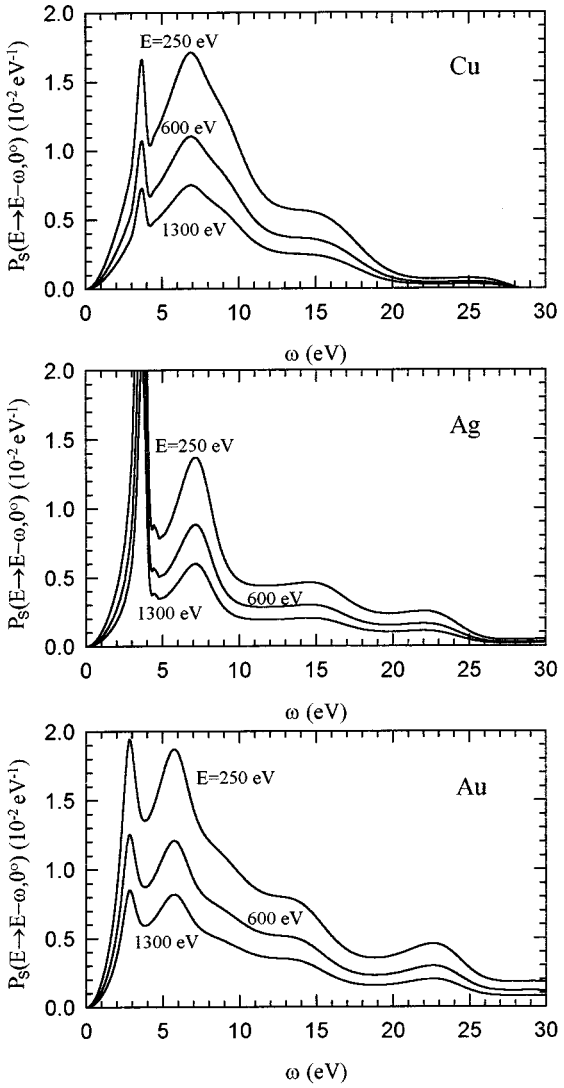

FIG. 2. A plot of the DSEP's for normal escape electrons of several energies in Cu, Ag, and Au.

Figure 3 shows a plot of the SEP's as a function of the angle between emission direction and the surface normal α for 500-eV electrons in Cu, Ag, and Au. The sharp increase of the SEP's at large angles indicates that the surface excitations are most probable for near-grazing electrons. This angular dependence has been verified experimentally for large-α values.[39]

With the obtained DIMFP and DSEP, we have calculated the response functions using the FFT algorithm. Figure 4 shows the results of these calculations (solid curves) for 500-eV electrons that are emitted in different directions from Cu. Also plotted in this figure are the results without surface excitations (dashed curve). This shows that the contribution from surface excitations to the response function is significant for energy loss in the region below 30 eV. This is consistent with the results of the DSEP's in Fig. 2. It is also seen that the influence of surface excitations is relatively more important at larger escape angles due to the increased surface excitation probability at these angles, as shown in Fig. 3.

Applying the response functions to the recursion formula of Eq. (44), we have evaluated the primary XPS spectra. Figures 5–7 show the primary excitation spectra of Cu 2*p*, Ag 3*p*, and Au 4*d* (solid curves) determined from the experimental Al/$K\alpha$-excited photoelectron spectra (dashed curves).[17] For comparison, we also plot the corresponding results given by Tougaard (chain curves),[17] who neglected surface excitations. It is found that essentially all intensity far away from a peak is consistently removed. In all cases studied the present results are markedly different from Tougaard's results, which have a tail extending ~50 eV below the peak. It is seen that the tail can almost be removed when the surface excitations are considered. Therefore, the large tail which occurred in Tougaard's results is not part of the primary excitation spectrum, but may be due to inelastically scattered electrons caused by surface excitations.

The solid curves in Figs. 5–7 still accompany tiny tails. With respect to the solid-state effect, Doniach and Sunjic[40] suggested that a single-electron excitation induces a shake-off process for metals called the Doniach-Sunjic process. Penn[41] has also pointed out that, theoretically, the intrinsic

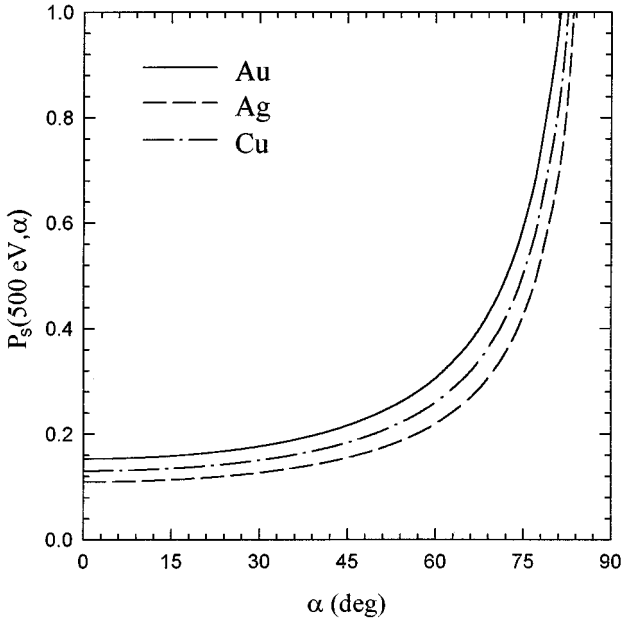

FIG. 3. A plot of the SEP's as a function of the angle between electron velocity and solid surface normal α for 500-eV electrons in Cu, Ag, and Au.

plasmon loss leads to another shake-off. The Doniach-Sunjic process cannot apparently account for the appearance of these tiny tails. It is also not effective to interpret these tiny tails as derived from intrinsic plasmon or from the intrinsic interband transitions. Therefore, more complete investigations are necessary to fully account for these tiny tails.

Figure 8 shows the result of a similar analysis of the photon-excited Ag (*MNN*) AES spectrum.[17] It reveals that the influence of surface excitations on the photon-excited AES spectrum is in the region not only close to but also far away from the peak.

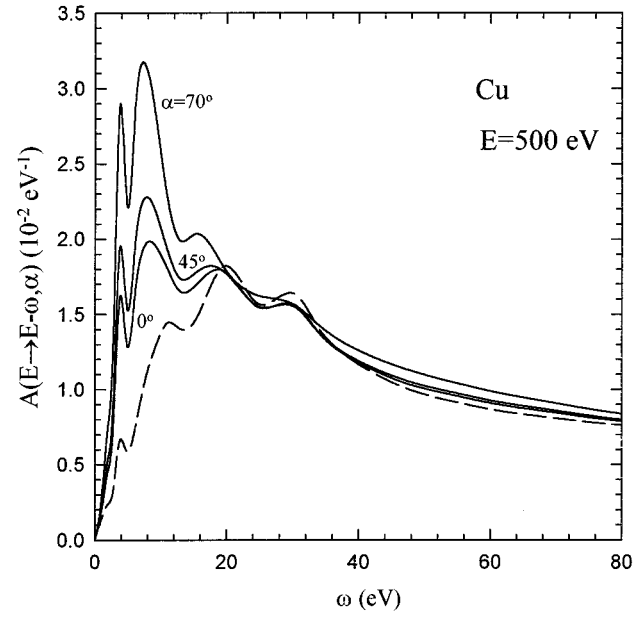

FIG. 4. A plot of the response function for 500-eV electrons of several escape angles in Cu. The solid and dashed curves, respectively, are results with and without surface excitations.

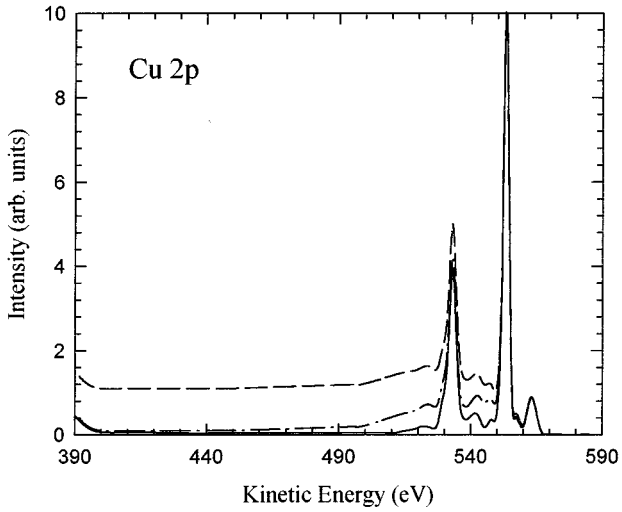

FIG. 5. The primary excitation spectrum of Cu 2*p* (solid curve) determined from the experimental Al $K\alpha$-excited photoelectron spectra (dashed curve) (Ref. 17). The chain curve is the corresponding result of Tougaard (Ref. 17).

Finally, it is worthwhile to mention that the present formulas for the surface excitations differ from the recent treatments by Yubero and Tougaard,[42] who included surface excitations in the analysis of REELS spectra. The authors assumed that an electron passes normally through a solid surface, and specular reflection in the backscattering event. For normally escaped angles, their results overestimate the contribution of surface excitations, because the detected electrons in XPS cross the surface once. In addition, their model was insufficient to describe the dependence of surface excitations on emission angles.

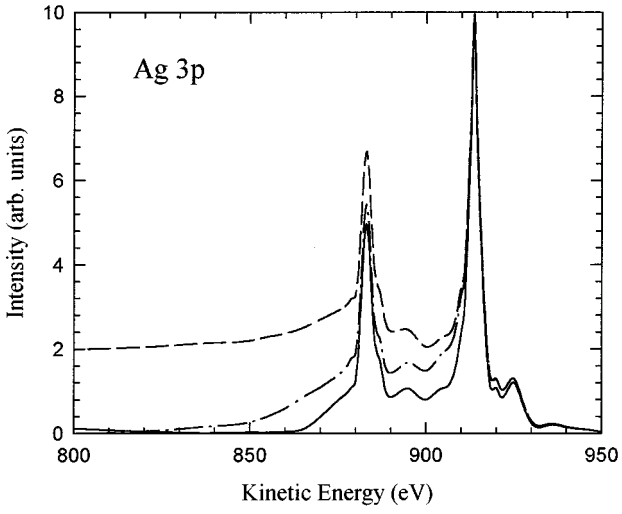

FIG. 6. The primary excitation spectrum of Ag 3*p* (solid curve) determined from the experimental Al $K\alpha$-excited photoelectron spectra (dashed curve) (Ref. 17). The chain curve is the corresponding result of Tougaard (Ref. 17).

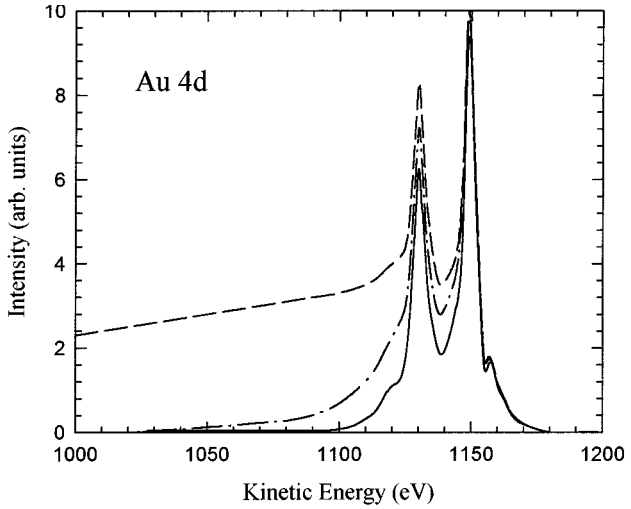

FIG. 7. The primary excitation spectrum of Au 4*d* (solid curve) determined from the experimental Al $K\alpha$-excited photoelectron spectra (dashed curve) (Ref. 17). The chain curve is the corresponding result of Tougaard (Ref. 17).

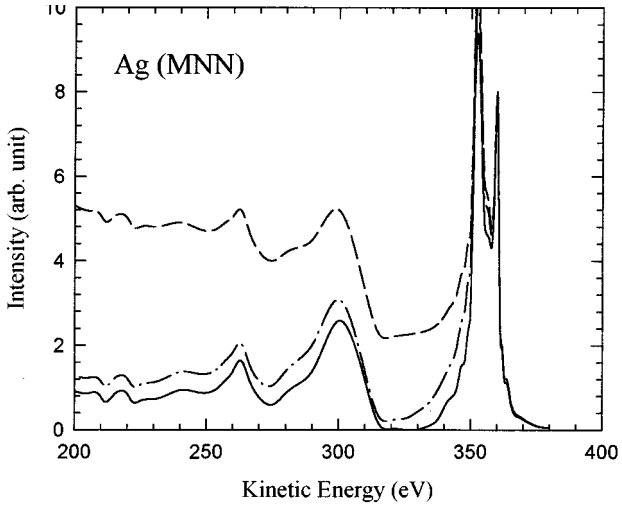

FIG. 8. The primary excitation spectrum of the photon-excited Ag (MNN) auger transition (solid curve) determined from the experimental Al $K\alpha$-excited photoelectron spectra (dashed curve) (Ref. 17). The chain curve is the corresponding result of Tougaard (Ref. 17).

V. CONCLUSIONS

We have included surface excitations in the Landau formula through Poisson statistics, and have derived a deconvolution formula in which the response function is in terms of the DIMFP and the DSEP. The influence of surface excitations on the background removal of electron spectra has also been studied. Through numerical calculations the primary XPS spectra of Cu, Ag, and Au were calculated from the experimental data. In all cases studied the present result is markedly different from Tougaard's result, which has a tail extending ~50 eV below the peak. It was seen that the large tail can be consistently removed when surface excitations are considered. In conclusion, the large tail which occurred in Tougaard's results is not part of the primary excitation spectrum but may be due to inelastically scattered electrons caused by surface excitations.

[1] D. P. Woodruff and T. A. Delchar, *Modern Techniques of Surface Science* (Cambridge University Press, New York, 1986).
[2] J. C. Riviere, *Surface Analytical Techniques* (Clarendon, Oxford, 1990).
[3] C. J. Powell, Surf. Sci. **44**, 29 (1974).
[4] M. P. Seah and W. A. Dench, Surf. Interface Anal. **1**, 2 (1979).
[5] C. M. Kwei, Y. F. Chen, C. J. Tung, and J. P. Wang, Surf. Sci. **293**, 202 (1993).
[6] J. T. Grant, T. W. Hass, and J. E. Houston, Phys. Lett. **45A**, 309 (1973).
[7] P. Staib and J. Kirschner, Appl. Phys. **3**, 421 (1974).
[8] D. A. Shirley, Phys. Rev. B **5**, 4709 (1972).
[9] H. H. Madden and J. E. Houston, J. Appl. Phys. **47**, 307 (1976).
[10] E. N. Sickafus, Surf. Sci. **100**, 529 (1980).
[11] M. F. Koenig and J. T. Grant, J. Electron. Spectrosc. Relat. Phenom. **33**, 9 (1984).
[12] S. Tougaard and P. Sigmund, Phys. Rev. B **25**, 4452 (1982).
[13] A. L. Tofterup, Phys. Rev. B **32**, 2808 (1985).
[14] V. M. Dwyer and J. A. D. Matthew, Surf. Sci. **193**, 549 (1988).
[15] A. L. Tofterup, Surf. Sci. **227**, 157 (1990).
[16] L. Landau, J. Phys. (Moscow) **8**, 201 (1944).
[17] S. Tougaard, Phys. Rev. B **34**, 6779 (1986).
[18] S. Tougaard and C. Jansson, Surf. Interface Anal. **20**, 1013 (1979).
[19] S. Tougaard and J. Kraaer, Phys. Rev. B **43**, 1651 (1991).
[20] H. Yoshikawa, R. Shimizu, and Z. J. Ding, Surf. Sci. **261**, 403 (1992).
[21] H. Yoshikawa, T. Tsukamoto, R. Shimizu, and V. Crist, Surf. Interface Anal. **18**, 757 (1992).
[22] D. D. Hawn and B. M. De Koven, Surf. Interface Anal. **10**, 63 (1987).
[23] R. H. Ritchie and A. L. Marusak, Surf. Sci. **4**, 234 (1966).
[24] F. Flores and F. Garcia-Moliner, J. Phys. C **12**, 907 (1979).
[25] D. Chan and P. Richmond, J. Phys. C **9**, 163 (1976).
[26] R. H. Ritchie, Phys. Rev. **106**, 874 (1957).
[27] R. F. Egerton, *Electron Energy-Loss Spectroscopy in the Electron Microscope* (Plenum, New York, 1986).
[28] H. Raether, in *Excitations of Plasmons and Interband Transitions by Electrons*, edited by G. Höhler, Springer Tracts in Modern Physics Vol. 88 (Springer, New York, 1980).
[29] R. H. Ritchie and A. Howie, Philos. Mag. **36**, 463 (1977).
[30] R. H. Ritchie, R. N. Hamm, J. E. Turner, H. A. Wright, and W. E. Bloch, in *Physical and Chemical Mechanisms in Molecular Radiation Biology*, edited by W. A. Glass and M. N. Varma (Plenum, New York, 1991), p. 99.
[31] D. Y. Smith and E. Shiles, Phys. Rev. B **17**, 4689 (1978).
[32] C. J. Tung, Y. F. Chen, C. M. Kwei, and T. L. Chou, Phys. Rev. B **49**, 16 684 (1994).
[33] Y. F. Chen, P. Su, C. M. Kwei, and C. J. Tung, Phys. Rev. B **50**, 17 547 (1994).
[34] S. Tougaard, Surf. Interface Anal. **11**, 453 (1988).

[35] A. A. Lucas, Phys. Rev. Lett. **26**, 229 (1971).
[36] E. Evans and D. L. Mills, Phys. Rev. B **5**, 4126 (1972).
[37] J. Schilling, Z. Phys. B **25**, 61 (1976).
[38] A. A. Lucas and M. Sunjic, Prog. Surf. Sci. **2**, 75 (1972).
[39] C. J. Powell, Phys. Rev. **175**, 511 (1968).
[40] S. Doniach and M. Sunjic, J. Phys. C **3**, 285 (1970).
[41] D. R. Penn, Phys. Rev. Lett. **38**, 1429 (1977).
[42] F. Yubero and S. Tougaard, Phys. Rev. B **46**, 2486 (1992).